

STAR FORMATION DURING GALAXY FORMATION

Bruce G. Elmegreen¹

Abstract. Young galaxies are clumpy, gas-rich, and highly turbulent. Star formation appears to occur by gravitational instabilities in galactic disks. The high dispersion makes the clumps massive and the disks thick. The star formation rate should be comparable to the gas accretion rate of the whole galaxy, because star formation is usually rapid and the gas would be depleted quickly otherwise. The empirical laws for star formation found locally hold at redshifts around 2, although the molecular gas consumption time appears to be smaller, and mergers appear to form stars with a slightly higher efficiency than the majority of disk galaxies.

1 Introduction

In the first four lectures of this series, we reviewed star formation in local galaxies. Recall that the star formation rate is proportional to the CO emission, from which we concluded that star formation occurs only in molecular gas and that the consumption rate from molecules to gas is constant. This derivation assumed a fixed CO to H₂ conversion rate to get the molecular gas mass, a fixed IMF, uniform grain properties, and certain extinction corrections to get the star formation rate. In addition, the molecular fraction scales almost linearly with pressure, and the pressure depends on the mass column densities, Σ_{gas} and Σ_{stars} , and the velocity dispersions, σ_{gas} and σ_{stars} . We also saw that spiral waves promote star formation in the arms, or organize the star formation, but do not affect the average rate much. The same is apparently true for star formation in shells, bright rims and pillars, which trigger star formation in these regions, i.e., organize where it happens, without changing the global average rate much. Star formation seems saturated in inner disks, so the detailed mechanisms of cloud formation do not appear to matter.

¹ IBM T. J. Watson Research Center, 1101 Kitchawan Road, Yorktown Heights, New York 10598 USA, bge@us.ibm.com

In addition, we saw that stars form in hierarchical patterns with star complexes, OB associations, clusters, and so on, because of turbulence compression and self-gravity. As a result, there are power-law mass functions for clouds, clusters, and stars, and there are space-time correlations for clusters. There are probably similar space-time correlations for young stars which are not observed yet.

We would like to discuss here what changes for young galaxies at high redshift. At first, we expect high redshift galaxies to look like normal galaxies viewed in the restframe ultraviolet. They would look dimmer because of cosmological surface brightness dimming, and the star formation regions would be blurred out because of poor spatial resolution. But still, we might expect to see the uv restframe versions of normal galactic features, i.e., exponential disks, spiral arms, bars, lots of small star-forming regions, and a general diversity in the relative prominence of disks and spheroids (i.e., the Hubble types).

Barden, Jahnke & Häussler (2008) made model images of redshifted SDSS galaxies to $z = 0.15, 0.5$, and 1, and even increased the intrinsic brightness for the $z = 1$ images. The result was a significant loss of faint structures, including the outer disk and the faint star-forming regions. Overzier et al. (2010) redshifted “Lyman Break Analogs” to $z = 2, 3$, and 4. They found that small clumps blend together and faint peripheral tidal features disappear. Petty et al. (2009) looked at the standard structural measures: the Gini coefficient, M20 (central concentration), and the Sersic index for redshifted local galaxies. They found that the model galaxies were smoother (lower Gini) and more centrally concentrated (lower M20) than their local counterparts. These studies reinforce our notion that high redshift galaxies should look somewhat smooth and centrally concentrated if they are at all like local galaxies.

In fact, when deep high resolution images of the sky were taken, particularly by the Hubble Space Telescope (HST), disk galaxies did not look anything like these expectations from local galaxies. Beyond $z \sim 2$, galaxies are mostly irregular, asymmetric, and clumpy (van den Bergh et al., 1996; Abraham et al., 1996; Conselice et al., 2005). In particular, there is a class of galaxies that is almost entirely clumpy, with nearly half of the light in several big star-forming clumps and no obvious underlying exponential disk (Elmegreen & Elmegreen, 2005). Figure 1 shows two examples of clumpy disks, with UDF catalog numbers indicated. On the left are SkyWalker¹ images using the ACS camera and on the right are NICMOS images in the near-infrared with $3\times$ lower resolution. The galaxies contain several large star-forming clumps with no central concentration from a bulge or exponential disk.

In a catalog of galaxy morphologies in the HST Ultra Deep Field, considering only galaxies larger than 10 pixels so their internal structure can be observed, Elmegreen et al. (2005a) recognized 6 basic types: Chain galaxies (121 examples), Clump Clusters (192), Double (134), Tadpole (114), Spiral (313), and Elliptical (129). Only the spirals and ellipticals resemble local galaxies, and even then

¹designed by K. Jahnke and S.F. Sánchez, AIP 2004

the spirals tend to have bigger star-forming regions than local spirals and the ellipticals are clumpy as well (Elmegreen et al., 2005b). Photometric redshifts of these galaxies (Elmegreen et al., 2007a) suggested that all of the clumpy types extend out to at least $z \sim 5$ with extreme starburst spectral energy distributions. The spirals and ellipticals end at about $z \sim 1.5$, which could be because either their number density drops, or they are too faint in the restframe uv to see at higher redshifts.

2 What are the Clumpy Types?

Chain galaxies were originally identified by Cowie, Hu & Songaila (1995) using ground-based images. They are linear objects with several giant clumps along their length. There is often no central red clump, and no exponential profile as in a modern edge-on spiral galaxy. There are also many oval-shaped clumpy galaxies that resemble chains in having the same numbers, magnitudes, and colors for the clumps. More important, the relative numbers of these systems, chains versus clumpy galaxies, is consistent with the chains being edge-on clump clusters (Elmegreen et al., 2004a; Elmegreen & Elmegreen, 2005). Thus we have a new morphological type of galaxy, a thoroughly clumpy disk viewed in random

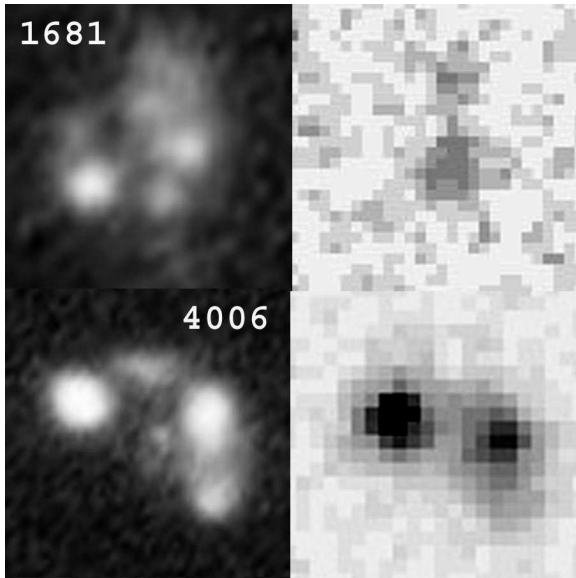


Fig. 1. Two examples of clump cluster galaxies from the HST UDF with color ACS camera images on the left and NICMOS images on the right (from Elmegreen et al., 2009a). These galaxies are characteristic of this class, having several large clumps of star formation and no obvious interclump disk.

orientations, that occurs primarily at high redshift.

Chains and clump clusters are so common that all modern spirals could have gone through this phase at $z > 1$. Essentially all observed disk systems are very clumpy at $z > 2$. The comoving space density of chains and clump clusters larger than 10 pixels in the UDF is $\sim 4 \times 10^{-3} \text{ Mpc}^{-3}$ for $z < 1$, decreasing to $\sim 1 \times 10^{-3} \text{ Mpc}^{-3}$ out to $z \sim 3$ or more. For spirals larger than 10 pixels in the UDF, the space density is $4 \times 10^{-3} \text{ Mpc}^{-3}$ for $z < 1$, but decreasing faster with z than the clumpy types, perhaps, in part, because spirals become too red to see. Considering also that the clumpy phase is probably shorter lived than the spiral phase, the prevalence of clumpy disks at high redshift seems clear.

Most clumps are not a bandshifting artifact of rest-UV normal star formation. Clumpy and spiral types are both present at low redshift. In GOODS, there are four basic types of disk galaxies: density wave spirals and flocculent spirals resembling today's galaxies, clumpy galaxies with a red disk between the clumps, and clumpy galaxies without any evident disk between the clumps. All four types span the same range of redshifts up to $z \sim 1$. There are clump clusters even at $z \sim 0.2$. This is such a low redshift that the observed V band in GOODS corresponds to a restframe passband of B band. Local spirals do not look like clump clusters in B band, so the clumpies are intrinsically different.

3 Mergers

Highly irregular massive disk galaxies in the local universe are usually mergers or interacting systems. We don't know if this is also true at high redshift. In the GOODS sample, there are clump clusters and chains at low redshift that look the same as those at high redshift in the UDF. But also in GOODS there are many examples of mergers and interactions that look like their local counterparts (Elmegreen & Elmegreen, 2006a; Elmegreen et al., 2007b). Thus normal mergers and interactions show up just fine in GOODS, and clump clusters are different. Clump clusters usually have no tidal features, for example, and they do not typically have double red nuclei from formerly separate galaxies.

Mergers are also not required to make a galaxy lopsided. Internal processes can do that too. Bournaud et al. (2008) observed a lopsided clump cluster in the UDF with Sinfoni. They found that it has a smooth rotation profile and metallicity gradient, so it does not look like a chaotic merger or have a double rotation curve. A simulation of this system reproduced the lopsided shape very well if the initial disk and halo were offset from each other a little. This offset seems reasonable if very young galaxies undergo rapid accretion from a cosmological inflow; they should often have their disk center-of-mass at a slightly different position than their halo center-of-mass. The disk mass in this model was $6 \times 10^{10} M_{\odot}$, with half of the disk mass in gas.

The final piece of evidence that chains are edge-on clump clusters is that the clumps in chain galaxies are highly confined to the midplanes. Their resolution-corrected rms deviation from the midplane of the chains is less than 100 pc (Elmegreen & Elmegreen, 2006b). This requires *in situ* clump formation, not

extra-galactic clump accretion. Also some chains are curved and not straight, and the clumps in them follow the curvature too, without significant deviations (Elmegreen & Elmegreen, 2006a). These may be interacting edge-on clumpy galaxies, but still the clumps formed in them and are not separate merger remnants.

4 Clump Cluster Properties

Clumpy young galaxies, whether somewhat face-on and called “clump clusters,” or edge-on and called chains, have properties that are consistent with their youth, and also show variations that are consistent with their gradual evolution into modern disks.

Their youthful appearance is reinforced by the observation that they are highly molecular (Tacconi et al., 2010; Daddi et al., 2008, 2010a) and highly turbulent (Förster Schreiber et al., 2009; Law et al., 2009, see below). Presumably the turbulence is a result of energy gained from intergalactic accretion (Elmegreen & Burkert, 2010) and gravitational instabilities in the disk (Bournaud, Elmegreen & Martig, 2009). Many young galaxies have a ratio of rotation speed to twice the dispersion speed that is less than unity. Förster Schreiber et al. (2009) consider that when this ratio is less than 0.4, the disks are dispersion-dominated. Their galaxies have stellar masses in the range from $10^{10} M_{\odot}$ to $10^{11} M_{\odot}$ and dynamical masses that are 3 to 5 times larger, on average.

Tacconi et al. (2010) made CO (3-2) maps of several clump clusters and found that typical clumps in these galaxies have $5 \times 10^9 M_{\odot}$ of H_2 with radii $< 1\text{-}2$ kpc, $\Sigma_{H_2} = 300 - 700 M_{\odot} \text{ pc}^{-2}$, and $\sigma \sim 19 \text{ km s}^{-1}$. They also derived a high gas fraction in the disks. Daddi et al. (2010a) observed CO in 6 galaxies at $z \sim 1.5$, finding rotation in some cases and a generally high gas fraction. The timescales for gas consumption, stellar build-up, and galactic dynamics were all comparable in the Daddi et al. study, which implies that the galaxies are very young. Daddi et al. also found that the efficiency of star formation is about the same as in normal galaxies today.

The clump stellar masses in clump clusters are ~ 100 times larger than star complex masses in modern spiral galaxies of similar luminosities (Elmegreen et al., 2009b). Bulges or bulge-like objects in clump clusters and chains are sometimes observed, and they are more like the clumps in terms of mass and age than are the bulges in spiral galaxies (Elmegreen et al., 2009a). The interclump surface density and age relative to the clump surface density and age also show variations among different clump clusters (Elmegreen et al., 2009b). All of these variations suggest an evolution from highly clumpy, bulge-free galaxies to smooth spiral galaxies with bulges.

There are essentially no barred clump cluster galaxies. Even if bars were present, they could hardly be recognized in such irregular disks. Bars appear only when the galaxies calm down and develop exponential disks and central concentrations or bulges. Still, there are elongated clumps in some clump clusters, suggesting protobars (Elmegreen et al., 2004b). If these objects really turn into bars, then this suggests bar formation can be a gas-rich process, including signif-

icant energy dissipation, and not a pure stellar process as in standard numerical models.

5 Working Model

The most likely model for the origin of clumps in clumpy galaxies is that they form by gravitational instabilities in rapidly assembled disks. The clumps are confined to within 100 pc of the mean disk, they are young star-forming regions (not diverse merged galaxies), the clump masses are $10^7 M_\odot - 10^8 M_\odot$, sometimes $10^9 M_\odot$, and these masses appear to be the ISM Jeans masses with the measured turbulent speeds and gas column densities. For example, $M_{\text{Jeans}} \sim \sigma^4 / G^2 \Sigma \sim 10^8 M_\odot$ if $\sigma \sim 30\text{--}50 \text{ km s}^{-1}$ and $\Sigma_{\text{gas}} \sim 100 M_\odot \text{ pc}^{-2}$. These dispersions are consistent with observed HII dispersions (Förster-Schreiber et al., 2006; Förster Schreiber et al., 2009; Weiner et al., 2006; Genzel et al., 2006, 2008; Puech et al., 2007; Law et al., 2009) and this column density is typical for the inner disk regions of spiral galaxies today. It is also comparable to what Tacconi et al. (2010) observed directly using CO emission.

There are many consequences of having such large clumps in a galaxy disk (Noguchi, 1999; Immeli et al., 2004a,b; Bournaud, Elmegreen & Elmegreen, 2007). They contribute strongly to the total disk potential, so they interact gravitationally, experience strong dynamical friction, and lose angular momentum to the outer disk. This all causes them to migrate rather quickly to the disk center where they contribute to a growing bulge (Elmegreen et al., 2008a). Star formation in the center can get triggered by their merger too, and this adds to the bulge. At the same time, their disruption in the disk causes it to smooth out, and this, combined with their angular momentum transfer, gives the disk an exponential radial profile (Bournaud, Elmegreen & Elmegreen, 2007). All of this disk evolution can happen within 0.5-1 Gyr.

Stirring from the clumps also thickens the disk and this probably produces the thick disk component of today's spiral galaxies (Bournaud, Elmegreen & Martig, 2009). Thick disks can also form by minor mergers, both through the stirring of existing disk stars and the dispersal of the merger remnants (Quinn et al., 1993; Walker et al., 1996). However, thick disks formed in this way flare out at the edge, and real thick disks do not seem to do this (Yoachim & Dalcanton, 2006; Bournaud & Elmegreen, 2009). Stirring by internal processes automatically makes a thick disk with an approximately constant scale height, because the stirring force from clump gravity is proportional to the disk restoring force from gravity. In the case of a merger, the stirring force is proportional to the companion galaxy mass and independent of disk restoring force, so the disk is dispersed much further in the outer regions than the inner regions (Bournaud & Elmegreen, 2009).

There is also a possible connection with nuclear black holes if the dense clusters that are likely to be present in the cores of the individual disk clumps form intermediate mass black holes by stellar coalescence, as proposed for dense clusters by Ebisuzaki et al. (2001), Portegies-Zwart & McMillan (2002), and others. If the clumps form black holes in this way, then these black holes will migrate

into the disk center along with the clumps, and possibly merge to make a massive nuclear black hole. Simulations of this process obtain a correlation between the black hole mass and the bulge velocity dispersion that is similar to what is observed (Elmegreen et al., 2008b). If the clumps make globular clusters too (Shapiro et al., 2010), then the correlation between globular cluster number and central black hole mass (Burkert & Tremaine, 2010) might be explained in the same way.

6 Stream-fed Disks

Galaxy accretion by cold gas streams is a way to feed gas into the disks fast enough to produce wild instabilities and clump formation. This can all happen without galaxy mergers, except for some small galaxy-like pieces that come in with the cold flows. The recognition of cold flows is a major change in thinking about how galaxies form (Murali et al., 2002; Birnboim & Dekel, 2003; Semelin & Combes, 2005; Dekel & Birnboim, 2006; Ocvirk et al., 2008; Dekel et al., 2009a,b; Agertz et al., 2009; Kereš et al., 2005, 2009; Brooks et al., 2009). Hierarchical build-up models in the cold dark matter scenario may not apply to baryons as much as they apply to cold dark matter itself. The baryons may enter a galaxy in the form of cold flows, rather than minor and major mergers of component galaxies, each with their own dark matter halo.

Ceverino, Dekel & Bournaud (2010) modeled cold and hot flows with a disk galaxy forming in the center. The model is appropriate for a redshift of $z = 2.3$. They follow the formation and evolution of individual clumps in the disk gas, showing how the accretion quickly makes an unstable gas disk, which forms giant clumps that migrate to the center.

7 Local analogs of clumpy galaxies

Clumpy galaxies do not look like local galaxies even when the local galaxies are modified to appear as they would at high redshift. FUV images of local galaxies contain too many star-forming clumps, and they are also more centrally concentrated than clump clusters. Spiral and barred structure in local galaxies would still show up at high redshift too (using the HST ACS camera, for example), if the disk is not too faint to see.

UDF clump clusters have bigger and fewer clumps than local galaxies, even in the restframe uv, they have no symmetry or central concentration, and they are much brighter in restframe magnitudes. Typical clump clusters have surface brightnesses that are more than 10 times larger than the surface brightness of, for example, M101, which is a locally bright galaxy with lots of giant star-formation clumps (although the M101 clumps are still small by high redshift standards).

We may wonder if local flocculent spiral galaxies are a better match to high- z galaxies because local flocculents get most of their structure from gravitational instabilities in the gas and there are no prominent spiral waves in the old stellar disk. Two redshifted versions of the flocculent galaxy NGC 7793 were shown in

Elmegreen et al. (2009b) and compared to GEMS galaxies. The local and distant galaxies do not look similar at all. In general, local galaxies are too smooth and too centrally concentrated compared to clump clusters.

On the other hand, a local dwarf Irregular galaxy is a good match to a clump cluster, although the clump clusters are much more massive (Elmegreen et al., 2009b). Clump clusters resemble local dwarf irregulars because both have high gas fractions, both have big complexes relative to the galaxy size, both have relatively thick disks, and both have high velocity dispersions relative to the rotation speed. Recall that $L_{\text{Jeans}}/\text{GalaxySize} \sim H_{\text{disk}}/\text{GalaxySize} \sim (\sigma/V)^2$. That is, the clump size from gravitational instabilities is comparable to the galactic scale height, and the ratio of these lengths to the galaxy size is the square of the ratio of the velocity dispersion to the rotation speed. Thus big complexes, thick disks, and high dispersions (relative to galaxy size and rotation speed) all go together regardless of the galaxy mass.

Both local dwarf irregulars and clump clusters are irregular because they have a relatively high gas mass and a high σ/V . Both are also relatively young in terms of the number of rotations they have lived and in terms of the relative gas abundance. The resemblance between clump clusters and local dwarfs is another example of down sizing: small galaxies today (dwarf irregulars) are doing what big galaxies (clump clusters) did at $z \sim 2$ (Elmegreen et al., 2009b).

There are other local galaxies that resemble clump clusters too, but they have about the same stellar mass as clump clusters, i.e., they are large galaxies. These local analogues are extremely rare, however. Casini & Heidmann (1976a,b) and Maehara et al. (1988) discovered local “clumpy irregular galaxies” of normal size. Examples are Markarian 296, 325, 7, 8 (which are ultraviolet galaxies), and Kiso UV excess galaxies 1618+378, 1624+404, 1626+413, and Mrk 297. Maehara et al. (1988) determined galactic distances of 60 to 120 Mpc, clump sizes of $\sim 2''$ (corresponding to 1 kpc), and clump absolute magnitudes of $M_B \sim -11$ to -16 mag (corresponding to $\sim 10^6 L_\odot$ to $10^8 L_\odot$).

Garland et al. (2007) studied Luminous Compact Blue Galaxies. These are small, high luminosity, high surface brightness galaxies with a blue color. They are also gas-rich (CO, HI), like high- z galaxies, and rotating with distorted velocities, as if they are interacting or lopsided. Overzier et al. (2008, 2009, 2010) studied Lyman Break Analogs (Heckman, 2005). These are super-compact uv-luminous galaxies. They are GALEX objects with $L_{\text{FUV}} > 10^{10.3} L_\odot$ and intensities $I_{\text{FUV}} > 10^9 L_\odot \text{ kpc}^{-2}$ at redshifts $z < 0.3$. They are also very rare ($\sim 10^{-6} \text{ Mpc}^{-3}$).

8 What should a Model of Star Formation be for High Redshift Galaxies?

Young galaxies look like their whole disk is out of equilibrium. In general terms, the star formation rate is expected to equal the accretion rate. This implies that if simple laws like the KS relation or the Bigiel-Leroy relation apply, then they fix the gas column density or molecular column density for a given star formation rate, not the other way around. Maybe the molecular abundance still depends

on pressure and the radiation field, and maybe stars still form only in molecular gas, but if the star formation rate is pinned to the accretion rate, then these local relations are not useful and in predicting the star formation rate. Perhaps the growth rate of GMCs equals the accretion rate by a whole galaxy. This would seem to be necessary to maintain a steady state. In a broad sense, this situation is like the dynamical triggering models discussed in these Lectures earlier, i.e., the spiral-wave or shell-like organization of gas into star-forming regions. Instead of spiral waves and shells collecting matter on a kpc scale, whole galaxies are collecting matter on a 10 kpc scale.

9 Comparison of Star Formation Models

Choi & Nagamine (2010) compared three models for star formation in cosmological simulations, the Springel & Hernquist (2003) model, the Blitz & Rosolowsky (2006) model, and the Schaye & Dalla Vecchia (2008) model. These are instructive to review here so that the diversity of analytical models can be noted.

In the Springel & Hernquist (2003) model, there is cooling gas with a star formation rate

$$d\rho_*/dt = (1 - \beta)\rho_c/t_{\text{SFR}}, \quad (9.1)$$

where β equals the supernova gas return fraction, ρ_c equals the density of cool clouds, $t_{\text{SFR}} = t_0^*(\rho/\rho_{\text{th}})^{-1/2}$ is the dynamical time, where $t_0^* = 2.1$ Gyr gives the local KS law. They also assumed $\Sigma_{\text{SFR}} = 0$ if $\Sigma < \Sigma_{\text{th}}$ for threshold column density Σ_{th} , and $\Sigma_{\text{SFR}} = A(\Sigma_{\text{gas}}/1 M_{\odot} \text{ pc}^2)^n$ for $A = 2.5 \pm 0.7 M_{\odot} \text{ yr}^{-1} \text{ kpc}^{-2}$, $n = 1.4$, and $\Sigma_{\text{th}} = 10 M_{\odot} \text{ pc}^{-2}$. This equation for star formation rate is combined with another equation for the rate of change of the cool cloud density,

$$d\rho_c/dt = C\beta\rho_c/t^*, \quad (9.2)$$

where $C = C_0(\rho/\rho_{\text{th}})^{-4/5}$. This assumes that supernovae evaporate and form cold clouds as in McKee & Ostriker (1977).

In the Blitz & Rosolowsky (2006) model, the molecular fraction is given by $\rho_{\text{H}_2}/\rho_{\text{HI}} = (P_{\text{ext}}/P_0)^{0.92}$, where $P_0 = 4.3 \times 10^4 \text{ k}_B \text{ K cm}^{-3}$. Then for a star formation rate, they assume

$$d\rho_*/dt = (\rho_{\text{gas}}/\text{Gyr})/[1 + (P + P_0/P_{\text{ext}})^{0.92}], \quad (9.3)$$

which assumes $\Sigma \propto \rho$ (a constant scale height). This star formation rate was applied only when $P_{\text{ext}} < P_0$. For $P_{\text{ext}} > P_0$, Choi & Nagamine (2010) used the Springel & Hernquist law (i.e., the Kennicutt $n = 1.4$ law).

The third model was that of Schaye & Dalla Vecchia (2008). These authors solved for the scale height using $\Sigma_{\text{gas}} = \rho_{\text{gas}}L_{\text{Jeans}} = (\gamma f_g P_{\text{tot}}/G)^{1/2}$, where γ is the adiabatic index: $P_{\text{tot}} \sim \rho_{\text{gas}}^\gamma$ (P_{tot} and ρ_{tot} include stars), f_g equals the gas mass fraction, and f_{th} equals the thermal pressure fraction ($P = f_{\text{th}}P_{\text{tot}}$). They assumed $f_g = f_{\text{th}}$, so if $\Sigma_{\text{SFR}} = A\Sigma_{\text{gas}}^n = \Sigma_{\text{gas}}/t$ which means $t = \Sigma_{\text{gas}}^{1-n}/A$, then $t_{\text{SFR}} = A^{-1}(M_{\odot} \text{ pc}^2)^n(\gamma P/G)^{(1-n)/2}$, and finally $d\rho_*/dt = \rho_{\text{gas}}/t_{\text{SFR}}$. Note

that in this model, $\Sigma_{\text{SFR}} \propto \Sigma_{\text{gas}} P^{0.2}$. They also assumed a threshold density, $\rho_{\text{th}} = \Sigma_{\text{th}}/L_{\text{Jeans}}$, so $\rho_{\text{th}} = \Sigma_{\text{th}}^2 G/c_s^2 f_g$ for $c_s = 1.8 \text{ km s}^{-1}$ (500K gas), and they assumed $P = K\rho^{4/3}$.

Choi & Nagamine (2010) note that the Springel & Hernquist model forms too many stars at low Σ_{gas} and this causes it to form stars too early in the Universe. The other models have a pressure dependence for star formation which gives an acceptably low rate in low pressure regions.

Genzel et al. (2010) reviewed the star formation and CO data for high- z galaxies in the context of the “main-sequence line” for star formation:

$$SFR(M_{\odot} \text{ yr}^{-1}) = 150(M_*/10^{11} M_{\odot})^{0.8}([1+z]/3.2)^{2.7} \quad (9.4)$$

(Bouche et al., 2010; Noeske et al., 2007; Daddi et al., 2007).

Genzel et al. noted that the gas depletion time depends weakly on z . It is $\sim 0.5 \text{ Gyr}$ at $z > 1$, and 1.7 Gyr at $z = 0$, while mergers have $2.5 - 7.5\times$ shorter depletion times than non-mergers. At $z > 1$, the depletion time is comparable to the stellar age, and it is always shorter than the Hubble time. This means there is a continuous need for gas replenishment in galaxy disks.

Genzel et al. also found that the molecular star formation-column density relation is in agreement with Bigiel et al. (2008). There is no steepening at $\Sigma_{\text{gas}} > 100 M_{\odot} \text{ pc}^{-2}$ like there appears to be in local starbursts. In general, they find no variation in the empirical star formation law with redshift.

The dynamical version of the Kennicutt (1998) relation was examined by Genzel et al. too. The dynamical relation says that the star formation rate is proportional to the gas column density divided by the local orbit time. Even in this form, mergers were found to be more efficient at star formation than non-mergers. The star formation efficiency per unit dynamical time was about 1.7%.

These considerations led Genzel et al. to a fundamental plane of star formation, in which the total galactic star formation rate depends only on the dynamical time and the total molecular mass:

$$\log\left(\frac{SFR}{M_{\odot}/\text{yr}}\right) = -0.78 \pm 0.23 \log\left(\frac{t_{\text{dyn}}}{\text{yr}}\right) + 1.37 \pm 0.16 \log\left(\frac{M_{\text{mol}}}{M_{\odot}}\right) - 6.9 \pm 1.9, \quad (9.5)$$

all with a standard deviation of 0.47 dex. This is the same as

$$SFR = 130 \left(\frac{M_{\text{mol}}}{10^{10} M_{\odot}}\right)^{1.37} \left(\frac{t_{\text{dyn}}}{100\text{Myr}}\right)^{-0.78} M_{\odot} \text{ yr}^{-1}. \quad (9.6)$$

Genzel et al. (2010) summarized the various star formation-density laws as follows. The Kennicutt slope of ~ 1.4 includes HI, whereas the Bigiel et al. (2008) slope of ~ 1 is just for CO (or H₂). Genzel et al. redid the Kennicutt (1998) slope of 1.4 with just H₂ and got a slope of ~ 1.33 . They redid their own relation for Σ_{SFR} versus Σ_{gas} including HI in addition to H₂ and found that it increases the slope from 1.17 to 1.28. Kennicutt (1998) used the same CO-H₂ conversion factor everywhere. When Genzel et al. redid the Kennicutt (1998) data with

a variable CO-H₂ conversion factor including only H₂, the slope increased from 1.33 to 1.42. Thus the inclusion of HI and the constant CO-H₂ conversion factor somewhat cancel each other in the Kennicutt (1998) relation. Genzel et al. (2010) also included new merger galaxies, which flatten the slope compared to that in Kennicutt (1998). Writing the star formation rate as $\Sigma_{\text{mol}}/t_{\text{dyn}}$ works fairly well, including both mergers and normal galaxies at all redshifts.

Daddi et al. (2010b) fitted Ultrahigh Luminosity Infrared Galaxies (ULIRGS) and Submillimeter Wave Galaxies (SMGs) to the same star formation-column density relation if the SF law is $\Sigma_{\text{SFR}} \sim \Sigma_{\text{gas}}/t_{\text{dyn}}$ (t_{dyn} is the rotation time at the outer disk radius). They suggested that the global star formation rate is proportional so $\sim (M_{\text{total gas}}/t_{\text{dyn}})^{1.42}$. High SFR galaxies consume their gas faster than a rotation time at the outer radius. This suggests that mergers are involved, or some other rapid accretion leading to centralized star formation.

10 Summary

Star formation at high redshift occurs in galaxies with high gas fractions and high turbulent speeds. The morphology is a clumpy disk without an exponential disk, bulge, or bar. There appear to be no exact local analogues, but what comes close are the dwarf Irregular galaxies, which are much lower in mass, along with very rare types called clumpy irregular galaxies, luminous compact blue galaxies, Lyman Break Analogs, etc.. All have a small number of giant star-forming regions, presumably because they are all gas-rich and highly turbulent. The main process of star formation everywhere seems to be gravitational instabilities. The clump masses are large and the rates are large because of the high turbulence and high gas mass fractions. There is a relation between the star formation rate and the galaxy mass versus redshift, called the “main sequence” line. Cosmological models have been made that fit this line fairly well. Generally, the Σ_{SFR} versus Σ_{mol} relation is similar to that in local galaxies, with a slight preference for a rate given by the galaxy dynamical time rather than the pure gas dynamical time. In galaxy accretion models, the star formation rate quickly becomes equal to the gas accretion rate. Presumably Σ_{mol} adjusts to accommodate or enforce this equilibrium.

References

- Abraham, R.G., van den Bergh, S., Glazebrook, K., Ellis, R.S., Santiago, B.X., Surma, P., & Griffiths, R.E. 1996, *ApJS*, 107, 1
- Agertz, O., Teyssier, R., Moore, B. 2009, *MNRAS*, 397, L64
- Barden, M., Jahnke, K., & Häussler, B. 2008, *ApJS*, 175, 105
- Bigiel, F., Leroy, A., Walter, F., Brinks, E., de Blok, W. J. G., Madore, B., & Thornley, M. D. 2008, *AJ*, 136, 2846
- Birnboim Y., & Dekel A., 2003, *MNRAS*, 345, 349

- Blitz, L., & Rosolowsky, E. 2006, ApJ, 650, 933
- Bouche, N., et al. 2010, ApJ, 718, 1001
- Bournaud, F., Elmegreen, B.G., & Elmegreen, D.M. 2007, ApJ, 670, 237
- Bournaud, F., Daddi, E., Elmegreen, B.G., Elmegreen, D.M., Nesvadba, N., Vanzella, E., Di Matteo, P., Le Tiran, L., Lehnert, M., & Elbaz, D. 2008, A&A, 486, 741
- Bournaud, F., & Elmegreen, B.G. 2009, ApJL, 694, 158
- Bournaud, F., Elmegreen, B.G., & Martig, M. 2009, ApJ, 707, L1
- Brooks, A. M., Governato, F., Quinn, T., Brook, C. B., & Wadsley, J. 2009, ApJ, 694, 396
- Burkert, A., & Tremaine, S. 2010, ApJ, 720, 516
- Casini, C., & Heidmann, J. 1976a, A&AS, 24, 473
- Casini, C., & Heidmann, J. 1976b, A&A, 47, 371
- Ceverino, D., Dekel, A., & Bournaud, F. 2010, MNRAS, 404, 2151
- Choi, J.-H., & Nagamine, K. 2010, MNRAS, 407, 1464
- Conselice, C. J., Blackburne, J. A., Papovich, C. 2005, ApJ, 620, 564
- Cowie, L., Hu, E., & Songaila, A. 1995, AJ, 110, 1576
- Daddi, E., et al. 2007, ApJ, 670, 156
- Daddi, E., Dannerbauer, H., Elbaz, D., Dickinson, M., Morrison, G., Stern, D., & Ravindranath, S. 2008, ApJ, 673, L21
- Daddi, E. et al. 2010a, ApJ, 713, 686
- Daddi, E. et al. 2010b, ApJL, 714, L118
- Dekel A., & Birnboim Y., 2006, MNRAS, 368, 2
- Dekel, A., et al. 2009a, Nature, 457, 451
- Dekel, A., Sari, R., & Ceverino, D. 2009b, ApJ 703, 785
- Ebisuzaki, T., et al. 2001, ApJ, 562, L19
- Elmegreen, B.G., Elmegreen, D.M., & Hirst, A.C. 2004b, ApJ, 612, 191
- Elmegreen, B.G., Elmegreen, D.M. 2005, ApJ, 627, 632
- Elmegreen, B.G., & Elmegreen, D.M. 2006b, ApJ, 650, 644

- Elmegreen, B.G., Bournaud, F., & Elmegreen, D.M. 2008a, *ApJ*, 688, 67
- Elmegreen, B.G., Bournaud, F., & Elmegreen, D.M. 2008b, *ApJ*, 684, 829
- Elmegreen, B.G., Elmegreen, D.M., Fernandez, M.X., & Lemonias, J.J., 2009a, *ApJ*, 692, 12
- Elmegreen, B.G., & Burkert, A. 2010, *ApJ*, 712, 294
- Elmegreen, D.M., Elmegreen, B.G., & Hirst, A.C. 2004a, *ApJ*, 604, L21
- Elmegreen, D.M., Elmegreen, B.G., Rubin, D.S., & Schaffer, M.A. 2005a, *ApJ*, 631, 85
- Elmegreen, D.M., Elmegreen, B.G., & Ferguson, T.E. 2005b, *ApJL*, 623, L71
- Elmegreen, D.M., Elmegreen, B.G. 2006a, *ApJ*, 651, 676
- Elmegreen, D.M., Elmegreen, B.G., Ravindranath, S., & Coe, D. 2007a, *ApJ*, 658, 763
- Elmegreen, D.M., Elmegreen, B.G., Ferguson, T., & Mullan, B. 2007b, *ApJ*, 663, 734
- Elmegreen, D.M., Elmegreen, B.G., Marcus, M., Shahinyan, K., Yau, M., & Petersen, M. 2009b, *ApJ*, 701, 306
- Förster-Schreiber, N. M., et al. 2006, *ApJ*, 645, 1062
- Förster Schreiber, et al. 2009, *ApJ*, 706, 1364
- Garland, C. A., Pisano, D. J., Williams, J. P., Guzmán, R., Castander, F. J., & Sage, L.J. 2007, *ApJ*, 671, 310
- Genzel, R. et al. 2006, *Nature*, 442, 786
- Genzel, R. et al. 2008, *ApJ*, 687, 59
- Genzel, R. et al. 2010, *MNRAS*, 407, 2091
- Heckman, T.M., 2005, *ApJL*, 619, 35
- Immeli, A., Samland, M., Westera, P., & Gerhard, O. 2004a, *ApJ*, 611, 20
- Immeli, A., Samland, M., Gerhard, O., & Westera, P. 2004b, *A&A*, 413, 547
- Kennicutt, R.C., Jr. 1998, *ApJ*, 498, 541
- Kereš, D., Katz, N., Weinberg, D.H., Davé, R. 2005, *MNRAS*, 363, 2
- Kereš, D., Katz, N., Fardal, M., Davé, R., & Weinberg, D. H. 2009, *MNRAS*, 395, 160

- Law, D.R., Steidel, C.C., Erb, D.K., Larkin, J.E., Pettini, M., Shapley, A.E., Wright, S.A. 2009, *ApJ*, 697, 2057
- Maehara, H., Hamabe, M., Bottinelli, L., Gouguenheim, L., Heidmann, J., & Takase, B. 1988, *PASJ*, 40, 47
- McKee, C. F., & Ostriker, J. P. 1977, *ApJ*, 218, 148
- Murali, C., Katz, N., Hernquist, L., Weinberg, D.H., & Davé, R. 2002, *ApJ*, 571, 1
- Noeske, K. G., et al. 2007, *ApJ*, 660, L47
- Noguchi, M. 1999, *ApJ*, 514, 77
- Ocvirk, P., Pichon, C., & Teyssier, R. 2008, *MNRAS*, 390, 1326
- Overzier, R.A., et al. 2008, *ApJ*, 677, 37
- Overzier, R. A. et al. 2009, *ApJ*, 706, 203
- Overzier, R.A., Heckman, T.M., Schiminovich, D., Basu-Zych, A., Goncalves, T., Martin, D.C., & Rich, R.M. 2010, *ApJ*, 710, 979
- Petty, S.M., de Mello, D.F., Gallagher, J.S., III, Gardner, J.P., Lotz, J.M., Mountain, C.M., & Smith, L.J. 2009, *AJ*, 138, 362
- Portegies-Zwart, S. F., & McMillan, S. L. W. 2002, *ApJ*, 576, 899
- Puech, M., Hammer, F., Lehnert, M. D., & Flores, H. 2007, *A&A*, 466, 83
- Quinn, P. J., Hernquist, L., & Fullagar, D. P. 1993, *ApJ*, 403, 74
- Schaye, J., & Dalla Vecchia, C. 2008, *MNRAS*, 383, 1210
- Semelin, B., & Combes, F. 2005, *A&A*, 441, 55
- Shapiro, K.L., Genzel, R., & Förster Schreiber, N.M. 2010, *MNRAS*, 403, L36
- Springel, V., & Hernquist, L. 2003, *MNRAS*, 339, 289
- Tacconi, L., et al. 2010, *Nature*, 463, 781
- van den Bergh, S., Abraham, R.G., Ellis, R.S., Tanvir, N.R., Santiago, B.X., & Glazebrook, K.G. 1996, *AJ* 112, 359
- Walker, I. R., Mihos, J. C., & Hernquist, L. 1996, *ApJ*, 460, 121
- Weiner, B. J., et al. 2006, *ApJ*, 653, 1027
- Yoachim, P. & Dalcanton, J. J. 2006, *AJ*, 131, 226